Proceedings of the 4rd International Conference on Mechatronics and Smart Systems
DOI: 10.54254/2755-2721/2026.32500

Research on Time-Space Characteristics of Safe Operation of High-Altitude Tethered Kites

Bo Hei[1*], Jiahao Qu[1]

[1]School of Aeronautics, Chongqing Jiaotong University, Chongqing, China
**Corresponding Author. Email: heibo220038@163.com*

Abstract. This paper studies the time-space characteristics of safe operation of high-altitude tethered kite arrays to solve the problem of airspace use efficiency, builds a dynamic model of tethered kites based on spherical coordinate system and a double-layer collision detection method for the kite and tether using the minimum enclosing ellipsoid, builds a cooperative control framework with three key parameters: initial distance (S), release time difference (Δt) and pitch angle difference (Δβ), uses MATLAB simulation to analyze how these parameters affect safe operation, the trajectory prediction error of the model is less than 7.8%, simulation results show that controlling Δt can create a safe time window, when S = 75 m, the safe time window is mainly between 22 s and 32 s, controlling Δβ can achieve vertical separation, when Δβ ≥ 9°, the safe distance can be reduced to 50 m, this study gives the control limits of time difference and pitch angle difference for safe range, forms an active prevention method of "use time or attitude to make up for small space" and provides a theoretical basis for compact layout of kite power plants.

Keywords: high-altitude tethered kite, time-space characteristics of safe operation, cooperative control framework, release time difference, pitch angle difference.

1. Introduction

High-altitude wind energy systems have become a research focus because they can get stable wind energy at higher altitudes [1-3]. The key part—high-altitude tethered kite—its safe and efficient operation is very important to use its advantages [4]. Different from traditional wind farms, kite units are less influenced by wake flow. The main problem of layout is to find safe and efficient 3D airspace for each unit [5-6]. The operation airspace of high-altitude tethered kite is a cone shape with the ground station as the anchor point. Its shape is decided by rope length and pitch angle. Pitch angle has a direct influence on the conflict between single machine performance and space use: small pitch angle can improve wind energy capture efficiency, but it will make safe airspace bigger and reduce the number of machines that can be used [7].

The collision risk of high-altitude tethered kite comes from its complex space movement and tether winding. Scholars at home and abroad have made progress in tether dynamics [8-10], trajectory optimization [11] and collision risk assessment. Among them, the collision detection method based on Reich model [12] has been widely used in UAV field [13-14], which provides

DOI: 10.54254/2755-2721/2026.32500

important reference for this study. However, the research on time-space cooperative control strategy for kite arrays is not enough.

Therefore, this paper focuses on the time-space characteristics of safe operation of high-altitude tethered kite. It builds a dynamic model and a double-layer collision detection algorithm, and establishes a cooperative control framework with distance (S), release time difference (Δt) and pitch angle difference (Δβ) as the core. Through simulation, it quantifies the influence of each parameter on collision characteristics, defines dynamic safe operation area, and provides technical support for large-scale safe operation of kite power generation system.

2. System modeling and time-space representation of high-altitude tethered kite

2.1. Dynamic trajectory of high-altitude tethered kite

To predict the flight trajectory of the kite effectively, a particle dynamic model based on spherical coordinates (r, θ, φ) [15] is established. In Figure 1, the kite position is described by radial distance r, polar angle θ and azimuth angle φ, and the heading angle χ defines the flight direction.

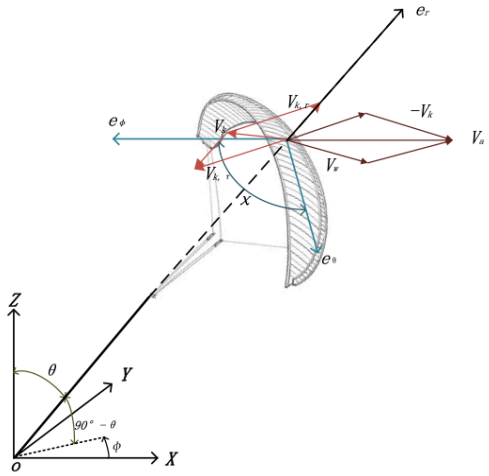

Figure 1. Kite reference coordinate system and velocity decomposition diagram

In spherical coordinates, the kite velocity v_k can be divided into radial wind speed v_{kr} and tangential wind speed v_{kt} components. The apparent wind speed v_a is defined as the vector difference between environmental wind speed v_w and kite velocity v_k [15]:

$$\overrightarrow{v_a} = \overrightarrow{v_w} - \overrightarrow{v_k} \tag{1}$$

Aerodynamic forces are calculated based on the apparent wind speed. Lift L and drag D are expressed as [16]:

$$L = \frac{1}{2}\rho A C_L \left|\overrightarrow{w}\right|^2 \tag{2}$$

$$D = \frac{1}{2}\rho A C_D \left|\overrightarrow{w}\right|^2 \tag{3}$$

DOI: 10.54254/2755-2721/2026.32500

where ρ is air density, A is kite area, C_L and C_D are lift and drag coefficients respectively.

2.2. 3D model for collision detection

To achieve accurate collision detection, this paper improves the traditional Reich model (cuboid) and uses the minimum enclosing ellipsoid to define the collision domain of the kite body, and discretizes the tether into equal-volume spheres. This method can describe the collision boundary more smoothly and avoid risk assessment oscillation caused by discontinuous curvature, as shown in Figure 2:

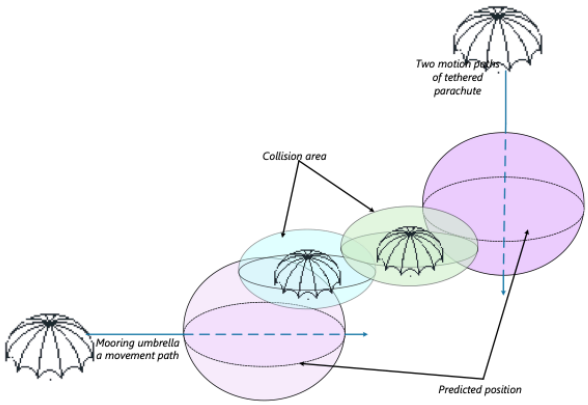

Figure 2. Collision area planning (original picture)

The geometric size of the kite is height 2h and maximum horizontal span a. The semi-height H and radius R of the enclosing ellipsoid are defined. The minimum circumscribed condition is obtained by optimization:

$$\frac{dV}{dH} = \frac{8\pi a^2(H^4-3H^2h^2)}{3(H^2-h^2)^2} = 0 \tag{4}$$

The optimal semi-axis parameters are obtained: $H_b = \sqrt{3}h, \quad R_b = \sqrt{3}a$. The algebraic equation of the corresponding ellipsoid collision area is:

$$\frac{(x-x_0)^2}{3a^2} + \frac{(y-y_0)^2}{3a^2} + \frac{(z-z_0)^2}{3h^2} \le 1 \tag{5}$$

$$p_i = \left(1 - \frac{i}{N}\right)p_a + \frac{i}{N}p_k \quad (i = 1, 2, \ldots, N) \tag{6}$$

$$d_{ij} = \sqrt{\frac{(x_i^{(2)}-x_j^{(2)})^2+(y_i^{(2)}-y_j^{(2)})^2}{+(z_i^{(2)}-z_j^{(2)})^2}} < 2D \tag{7}$$

The tether is discretized into N spheres with equal volume. A collision alarm is triggered when the ellipsoids of any two kites intersect, or the distance between the center of the kite ellipsoid and the sphere of a different tether segment is less than the safety threshold D. This model establishes a double-layer detection mechanism for the body and the tether.

DOI: 10.54254/2755-2721/2026.32500

2.3. Time-space definition of safe operation

The time-space definition of safe operation aims to ensure collision-free operation of the kite array in the whole cycle by quantifying the time and space constraint boundaries. For this purpose, three core controllable variables are selected to construct a cooperative control system: initial spacing S (horizontal distance between ground anchor points of adjacent kites) as the basic space constraint, which determines the degree of trajectory overlap; release time difference Δt (release interval between adjacent kites) adjusts the operation phase through asynchronous release, forms time dislocation in the dangerous space area, and constructs a "time safety window"; pitch angle difference Δβ (initial pitch angle difference between adjacent kites) establishes stable space isolation in the vertical dimension by assigning different reference heights to kites. Based on the actual deployment spacing S, this system derives two strategies for actively constructing safety boundaries: the control based on time difference changes the trajectory phase relationship by optimizing Δt, so that high-risk areas pass at different times; the control based on pitch angle difference realizes vertical stratification by maintaining Δβ to compensate for the lack of horizontal spacing. Together, they form an active prevention and control path of "insufficient space—time sequence/attitude compensation" to realize the dynamic construction and optimization of safe operation boundaries. The logic of dynamically constructing safety boundaries is shown in Figure 3:

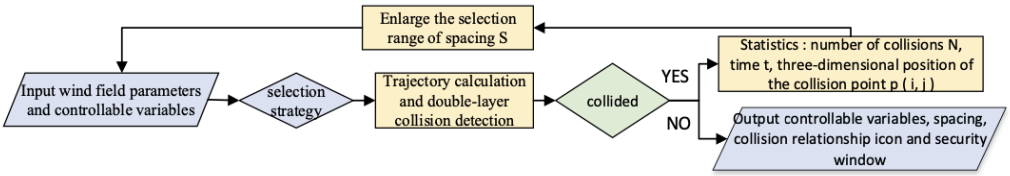

Figure 3. Logic of avoidance strategy

3. Verification of high-altitude tethered kite model

The simulation system is built based on MATLAB platform, integrating dynamic calculation, trajectory generation and collision detection modules. The double-layer algorithm of kite body and tether is used for collision detection. The main simulation parameters are shown in Table 1.

Table 1. Simulation input parameters

Wind speed v_w	8-12 m/s
Kite parameter A	25 m2
Tether length R	400 m
Tether division points n	100

To verify the accuracy of the model, the simulation trajectory is compared with the literature experimental data [17]. In Figure 4, the verification results show that the spatial coincidence degree between the model trajectory and the experimental data is more than 86%, and the trajectory prediction error at 9m/s wind speed is less than 7.8%, which proves that the model is reliable and supports the following analysis.

DOI: 10.54254/2755-2721/2026.32500

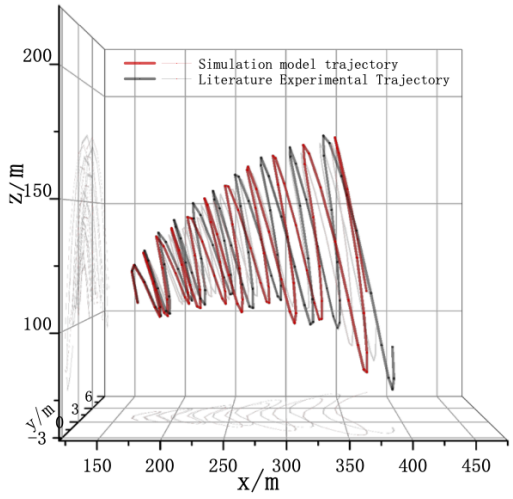

Figure 4. Comparison between simulation model trajectory and literature experimental trajectory

4. Research on time-space characteristics of high-altitude tethered kite

4.1. Regulation of release time difference

In Figure 5, synchronous release easily leads to trajectory overlap. The introduction of Δt can adjust the phase and realize time staggering. By comparing the collision results of synchronous release (Δt=0) and asynchronous release (Δt=9 s) under the working conditions of S=90 m and wind speed 10 m/s: 4 collisions occur in synchronous release, and 0 in asynchronous release, which verifies the effectiveness of time sequence regulation. The number of collisions fluctuates nonlinearly with Δt, and there is a safety window. Figure 6 shows the change of collision times under different Δt, and quantifies the safety interval of (S, Δt) combination. When S≥90 m, more than 75% of the Δt interval (0–40 s) is a safe area; when S=75 m, the safe Δt is concentrated in 22–32 s; when S=85 m, it expands to 10–36 s; when S≤65 m, only Δt=12–18 s is a very narrow safety window. The safety window width is positively correlated with S, which provides a quantitative basis for time sequence regulation under compact layout.

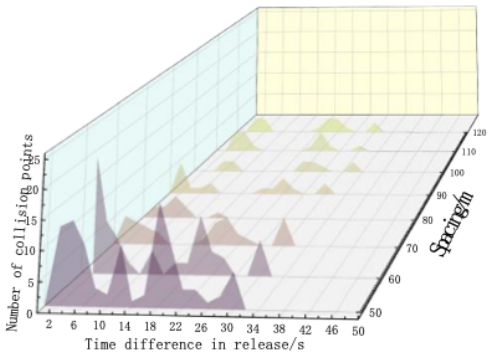

Figure 5. Collision result diagram with different release time differences

4.2. Regulation of pitch angle difference

In Figure 6, when the horizontal distance is not enough, vertical separation can be established by setting the initial pitch angle difference Δβ of adjacent kites. By comparing the effects of Δβ=2° and

DOI: 10.54254/2755-2721/2026.32500

Δβ=12° under the condition of S=60 m: when Δβ=2°, the trajectories overlap greatly and collisions happen frequently; when Δβ=12°, a stable height difference of about 32 m is formed and zero collision is achieved, which proves the strong robustness of attitude control. The systematic simulation in Figure 6 reveals the safety threshold of Δβ and its dynamic relationship with S. When Δβ<7°–8°, the collision risk is high; when Δβ≥11°–12°, zero collision can be achieved in the traction stage. The safety interval of (Δβ, S) combination is quantified: when Δβ≥4°, it can adapt to the conventional distance of S≥95 m; when Δβ≥9°, the safe adaptive distance can be reduced to S≥50 m; when Δβ<4°, only the super-large distance of S≥105 m can ensure safety. Increasing Δβ can effectively compensate for the lack of horizontal distance, providing a quantifiable attitude control criterion for compact deployment.

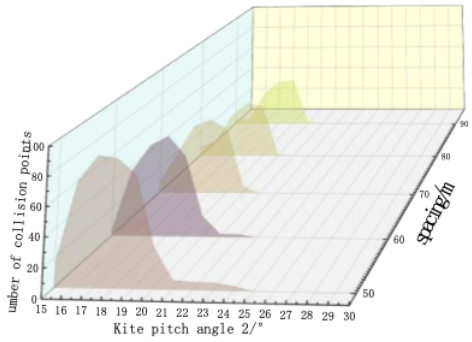

Figure 6. Collision result diagram with different kite pitch angles

5. Conclusion

This paper studies the time-space characteristics of safe operation of high-altitude tethered kites, constructs a dynamic model based on spherical coordinate system and a double-layer collision detection algorithm of kite body and tether, and establishes a cooperative control framework with initial spacing S, release time difference Δt and pitch angle difference Δβ as the core. The control rules of key parameters are quantified through MATLAB simulation. The main conclusions are as follows:

(1) The dynamic safe operation interval based on release time difference Δt is obtained. The safety window width is positively correlated with S: when S≥90 m, more than 75% of the Δt interval (0–40 s) is a safe area with high control fault tolerance; when S=75 m, the safe Δt is concentrated in 22–32 s; when S=85 m, it expands to 10–36 s; when S≤65 m, only Δt=12–18 s is a very narrow safety window. Time sequence control provides a directly applicable quantitative basis for kite arrays under compact layout.

(2) The safe operation interval based on pitch angle difference Δβ is clarified. Δβ is negatively correlated with S: when Δβ≥4°, it can adapt to the conventional distance of S≥95 m; when Δβ≥9°, the safe adaptive distance can be reduced to S≥50 m; when Δβ<4°, only the super-large distance of S≥105 m can ensure safety. Through vertical layered separation, attitude control can achieve zero collision operation in limited horizontal space, and gives quantifiable attitude control thresholds.

(3) A "time sequence-attitude" two-dimensional safe operation interval system is constructed, integrating two control paths of Δt and Δβ, breaking through the traditional passive protection mode relying on increasing physical distance, and forming an active prevention and control strategy of "insufficient space-time sequence/attitude compensation". This system can flexibly select the control mode according to the site distance constraint, significantly improve the airspace utilization on the

DOI: 10.54254/2755-2721/2026.32500

premise of ensuring zero collision, and provide systematic safe operation criteria and technical support for the large-scale and compact deployment of high-altitude tethered kite wind farms.

References

[1] Bechtle, P., et al. Airborne wind energy conversion systems: A review of the state of the art. Renew. Energy 2019, 141, 1103–1116.
[2] Han, S.; Liu, S. Distributed wind power generation technology based on high-altitude wind energy. Distrib. Energy 2024, 9, 1-9.
[3] Luchsinger RH. Pumping cycle kite power. In: Airborne wind energy. Springer; 2013. p. 47–64.
[4] Lian, Y., et al. A review of airborne wind energy systems: Modeling, control, and optimization. Ocean Eng. 2025, 323, 120643.
[5] Cobb, M., et al. A practical approach to airborne wind energy system design and control. IEEE Trans Control Syst Technol 2019, 28(4): 1447–1459.
[6] Reich, P. G. Analysis of aircraft separation minima using a collision risk model. J. Navigat. 1966, 19(1), 88–98.
[7] Zhang, H., et al. Collision risk assessment for multi-kite airborne wind energy systems. IEEE Access, 2022, 10, 103827–103839.
[8] Zou, Y., et al. Trajectory optimization and control of tethered kite for wind energy harvesting. IEEE Access, 2021, 9, 16630–16641.
[9] Johnson, H. Kite Farm Simulation. Delft University of Technology, 2019.
[10] Malz, E. C., et al. A reference model for airborne wind energy systems. Renew. energy, 2019, 140, 1004–1011.
[11] Yang, J. (2025). Research on wind farm layout optimization based on high-altitude kite dynamic trajectories (Master's thesis). Chongqing Jiaotong University.
[12] Argatov, I., et al. Energy conversion efficiency of kite-based airborne wind energy systems. Renew. Energy, 2008, 34(6), 1525–1532.
[13] Williams, P., et al. Modeling and control of tethered kites for wind energy generation. AIAA Modeling and Simulation Technologies Conference, 2007.
[14] Fuest, H., et al. Simulation and optimization of multi-kite airborne wind energy systems. CEAS Aeronaut. J., 2025, 16(1), 307–321.
[15] Schmehl, R., et al. Kite system modeling and control. In: Airborne Wind Energy, 2013, 23-45.
[16] De Lellis, M., et al. Feedback control of tethered kites for wind energy harvesting. Renew. energy, 2016, 86, 163–172.
[17] Ahrens U, Diehl M, Schmehl R, eds. Airborne Wind Energy [M]. Berlin: Springer, 2013.